Characterization of symmetric aberrations in aspheric surfaces using non-contact profilometry

Joseph Ellison* and Steven VanKerkhove
Corning Tropel Corporation, 60 O'Connor Road, Fairport, NY, USA 14450

ABSTRACT

A method for measuring symmetric aberrations in large departure aspheric surfaces to nearly single digit nanometer precision is demonstrated. Interferometry can accurately measure plano, spherical and small departure aspheric surfaces. However, null correction is normally required for accurate interferometric measurement of large departure aspheres. When using conventional null lenses, asymmetric aberrations are easily measured by simply rotating the surface under test to a finite number of positions and comparing them to one another. The rotationally symmetric errors are more difficult to know with certainty due to possible systematic rotationally symmetric errors with the null lens itself. The proposed system can measure aspheres on planar to f/6.0 spherical surfaces with a maximum sag of 1 mm and from 800 mm to 25 mm spherical surfaces down to f/0.55. A non-contact interferometric probe is used to measure the surface profile with the optic mounted on either a linear or rotary air bearing, depending on the base radius of curvature of the optic. Measurement results are shown for several aspheres and compared with interferometer measurements.

Keywords: Profilometry, non-contact, aspheric surface, symmetric aberrations

1. INTRODUCTION

High accuracy optical surface measurements are typically achieved using interferometric techniques. Resolutions in the single digit nanometer range are obtained for spherical optics under null testing conditions. However, interferometric testing of aspheric optics normally requires some sort of null corrector[1-3] to successfully resolve the dense fringe patterns. When using conventional null lenses, asymmetric aberrations are measured by rotating the surface under test to a finite number of positions and comparing them to one another. However, rotationally symmetric errors are more difficult to know with certainty due to possible systematic rotationally symmetric errors with the null lens itself. Also, null lenses can be expensive to fabricate and are designed for a specific asphere. Therefore, other test methods, interferometric, holographic and non-interferometric, have been devised to measure aspheres[4-6]. Non-null interferometer testing of aspheres is possible if the fringes can be resolved by the measurement system and the non-null effects of the imaging system are understood.[9-11]

Another approach used to measure aspheres is through the use of profilometry.[12-15] This method provides simple and accurate scans of the asphere with the possibility of mapping the whole surface. The degree of accuracy achievable is dependent on the type of probe used and the reference datum of the measurement system. The probe types are divided into two general areas; contact and non-contact probes. Contact probes are capable of highly accurate measurements but run the risk of damaging the surface. Therefore a non-contact measurement probe is preferable. In this paper, we develop a method for characterizing the symmetric aberrations of an aspheric surface using a non-contact probe. A single scan is obtained across the center of the aspheric surface. The part is translated while the probe is held fixed above the surface being scanned. The experimental setup, data processing of the surface measurements, discussion of the measurements results and comparison to interferometric measurements are presented in the following sections.

*ellisonjf@corning.com; phone 1 585 388-3580; fax 1 585 377-6332; tropel.com

2. SYSTEM DESCRIPTION

The measurement system is composed of a non-contact measuring probe and either a linear or rotary air bearing on which the part is mounted as shown in Figure 1. The non-contact probe is a fringe tracking, fizeau interferometer composed of a laser diode source, fiber optic cable and GRIN lens, control unit and PC computer. The non-contact probe measures the relative change in distance between the probe reference surface, fiber tip, and the part under test. The test part is translated or rotated while the non-contact probe remains stationary. The working distance for the probe is 15 mm with a range of +/- 1 mm. The angular range is +/- 5 degrees and is the limiting factor for deciding which setup the optic will be tested on, either the linear or rotary air bearing.

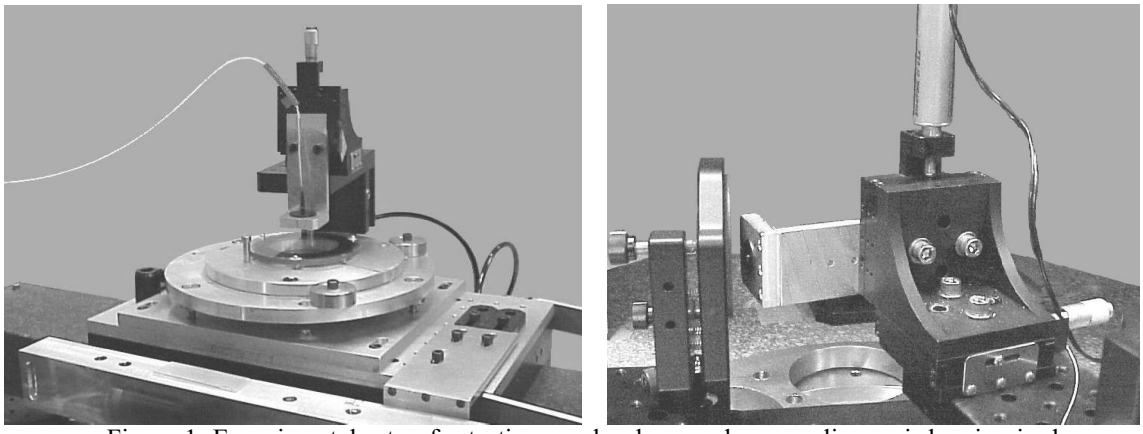

Figure 1: Experimental setup for testing nearly plano aspheres on linear air bearing is shown on the left and for spherical aspheres mounted on rotary air bearing is shown on the right.

The test part is placed on a kinematic tip/tilt plate on top of the linear air bearing stage. The plate provides for precise leveling and placement of the test part. The GRIN lens part of the probe is mounted on micrometer slides to allow exact positioning of the probe above the center of the test piece. Then as the part is translated under the probe, a surface scan through the center of the part is measured. The linear air bearing stage runs on a granite bar and is coupled to a motorized linear ball screw slide in such a way that only horizontal linear motion is transferred to the air bearing. This minimizes stage errors. A Heidenhain glass scale provides position of the linear air bearing stage. The whole assembly is mounted on an air-isolated table to minimize transmitted vibration and is in a temperature-controlled environment.

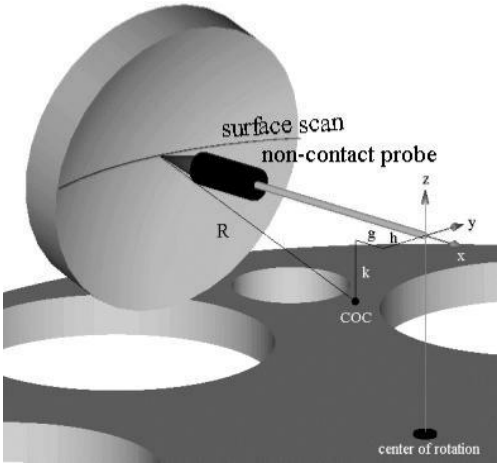

Figure 2: Typical setup on air bearing stage.

The rotary air bearing has an integral motor and encoder for precise rotation and position feedback. A vertical tip/tilt stage holds the test part and is mounted on a linear slide attached to the rotary stage. Again, the non-contact probe is mounted on micrometer slides. The non-contact probe is positioned to measure the surface profile through the center of the part as the part rotates on the air bearing. Figure 2 illustrates the probe placement relative to a concave test part. Sufficient degrees of freedom are available for aligning the test part center of curvature, COC, to the stage center of rotation thereby reducing the distances shown by g, h and k in the figure to zero. This setup is mounted on a large granite block to minimize transmitted vibration also in a temperature-controlled environment. Both the non-contract probe and encoder position are sampled and analyzed using a standard PC computer.

3. ERROR ANALYSIS

To maximize the reliability of surface profile measurement, it was necessary to minimize systematic errors in the final measurement. First, an understanding of the non-contact probe measurement error sources was acquired. Various test configurations were evaluated for the background noise when measuring with the probe. The results are tabulated in Table 1 for measurement scans of 10 seconds duration sampled at 500 Hz. The first three tests were performed with no motion; the probe and reference flat were stationary. The last two test cases represent measurements using typical run parameters for motion control. The reference flat used in the measurements was tested interferometrically and shown to have a low order surface error in the +/- 5 nm range. The same was true of the reference sphere. The results in the table are listed down the columns with relaxing constraints and increasing noise in the raw data. However, we were not interested in examining the high frequency features in the surface profile. Therefore, a low-pass filter with a cut-off frequency of 3 Hz for the stationary test conditions and 2 mm^{-1} for moving test conditions was applied. The overall noise level was consistently shown to be in the 6-7 nm range TIR and 1-2 nm RMS. The non-contact probe is then capable of resolving greater than 1 mm spatial features roughly 10-20 nm in height.

Table 1: Evaluation of background noise for non-contact probe for various configurations.

Description of probe setup	Raw Data		Filtered Data	
	TIR (nm)	RMS (nm)	TIR (nm)	RMS (nm)
Rigidly coupled to ref. flat	13.6	2.2	1.5	0.4
Above stationary ref. flat	28.6	4.8	6.5	1.3
Above stationary ref. flat with motor running	40.0	6.7	6.8	1.5
Above moving ref. flat	49.0	8.3	6.7	1.6
Next to rotating ref. sphere	93.0	16.0	5.8	1.3

A longer scan was measured to verify that there was no drift or low order error in the probe signal with time. A sample scan is illustrated in Figure 3.

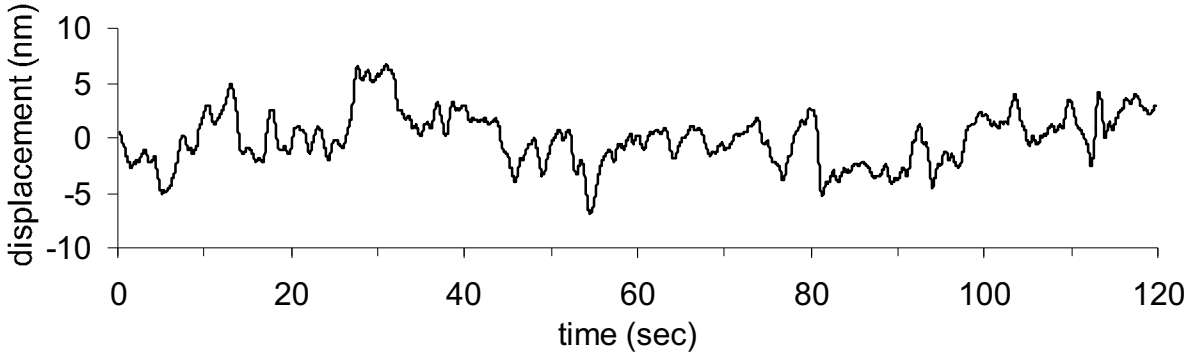

Figure 3: Noise and trending measured on linear air bearing with non-contact probe mounted over stationary reference flat with motor running.

Systematic errors of the linear slide were evaluated by measuring the reference flat surface. The reference flat was mounted on the kinematic plate on the linear air slide. Since the reference surface profile was known to be +/-5 nm from interferometer measurements, then any deviation from this could be attributed to slide error. The slide error was measured and shown in Figure 4 to be about 140 nm TIR over 160 mm of travel. In order to accurately remove this error from unknown surface measurements, the slide must repeat itself. Surface measurement repeatability was found to be +/-8 nm for 15 measurements. Positional errors related to not measuring through the center of the asphere are reduced by exact placement of the test part under the non-contact probe. The system resolution in placement of the surface is 13 μm, which is more than adequate since a 0.1 mm lateral offset results in a 1 nm error.

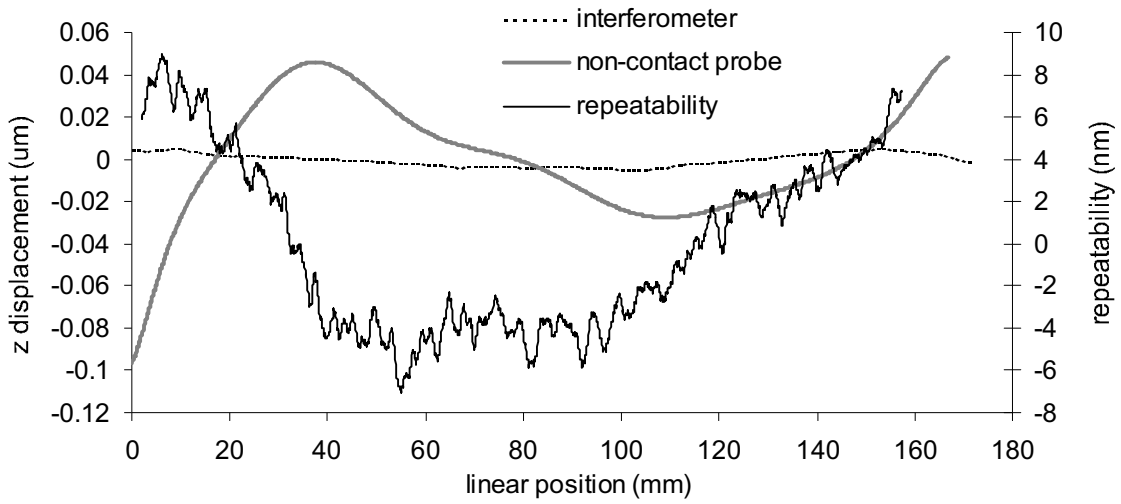

Figure 4: Linear air bearing slide error as measured with non-contact probe and reference flat. Reference flat has less than +/- 5 nm surface irregularity as shown by interferometer results. Slide error measurement to measurement variation is +/- 8 nm.

Systematic errors associated with the rotary air bearing were found to be less than 2 nm TIR over 50 degrees of rotation. Figure 5 compares an interferometer measurement of a reference sphere and the same reference measured

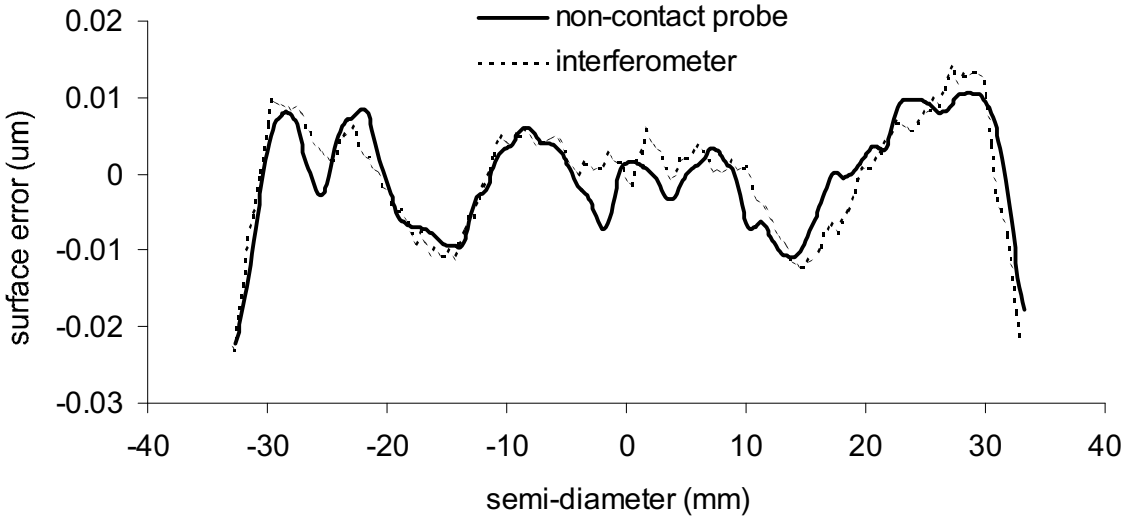

Figure 5: Measurement of reference sphere on rotary air bearing using non-contact probe as compared to interferometer measurement showing the systematic error in the air-bearing spindle.

on the rotary air bearing with the non-contact probe. The 2 nm oscillations in the probe results is due to the air bearing spindle. Repeatability was also better than +/-2 nm. Another possible source of measurement error deals with positional accuracy of the test part relative to the center of rotation of the air bearing. Figure 6 shows results from a sensitivity analysis of the positioning errors. It is desired that these errors be less than 1 nm. Design of the alignment controls on the measurement apparatus allows the positioning of the test part to a resolution of 1 μm in the radial direction, alignment of COC with the center of rotation, and 13 μm in the vertical direction, alignment of optic axis with center of rotation. Therefore, it is possible to accurately position the test part to achieve errors less than 1 nm.

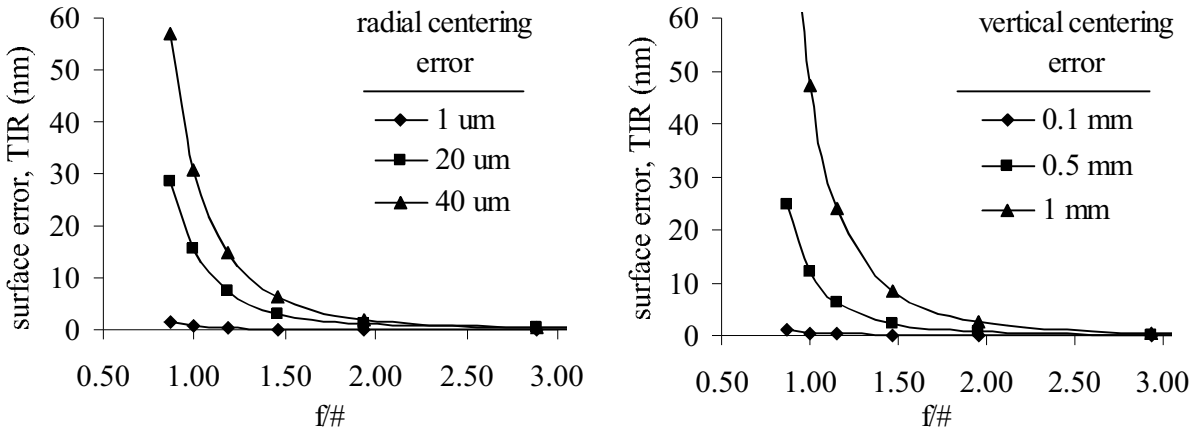

Figure 6: Surface error due to center of curvature not at air bearing center of rotation (defocus) and due to vertical offset of probe measurement location.

4. DATA PROCESSING METHOD

The following method has been developed to minimize asymmetric aberrations in the surface measurement. A single scan of the surface profile, $z(x_i)$, is measured across the center diameter of the test part. For the linear air bearing, the systematic slide error is subtracted from the surface scan. To find the measured center of the aspheric surface, the data is mirrored in the scan direction and subtracted. The difference is minimized in the least squares sense by shifting the data according to the equation

$$A = \min_{\substack{m \\ k}} \left[\sum_{i=0}^{m} \left(z_i - z_{m-i} \right)^2, \sum_{i=k}^{N} \left(z_i - z_{N-i} \right)^2 \right]. \tag{1}$$

Any anti-symmetric terms present in the data are then eliminated and asymmetries are reduced by mirroring the data around the measured center, x_c, using the minimized values from equation (1) and the following

$$z_i = \frac{\left(z_i - z_{m-i} \right)}{2} \tag{2}$$

where the measured center is given by

$$x_c = \frac{x_m - x_0}{2} \quad or \quad \frac{\left(x_N - x_k \right)}{2}. \tag{3}$$

The first or second equation of equation (3) is used based on which parameter, k or m, minimizes equation (1).

5. RESULTS

The above procedure was employed for the measurement of several aspheres. Each of the measurements was repeated several times. Figure 7 shows the comparison of a 10 μm asphere on a nearly planar surface that was measured using the suggested procedure and in transmission on a fizeau interferometer. There is some slight distortion in the interferometer measurement due to the large number of fringes in the high slope regions. It is in these areas that the largest deviation exists between the two measurements, roughly 45 nm. Code V modeling of the interferometer design verified that the interferometer was incapable of accurately imaging these areas.

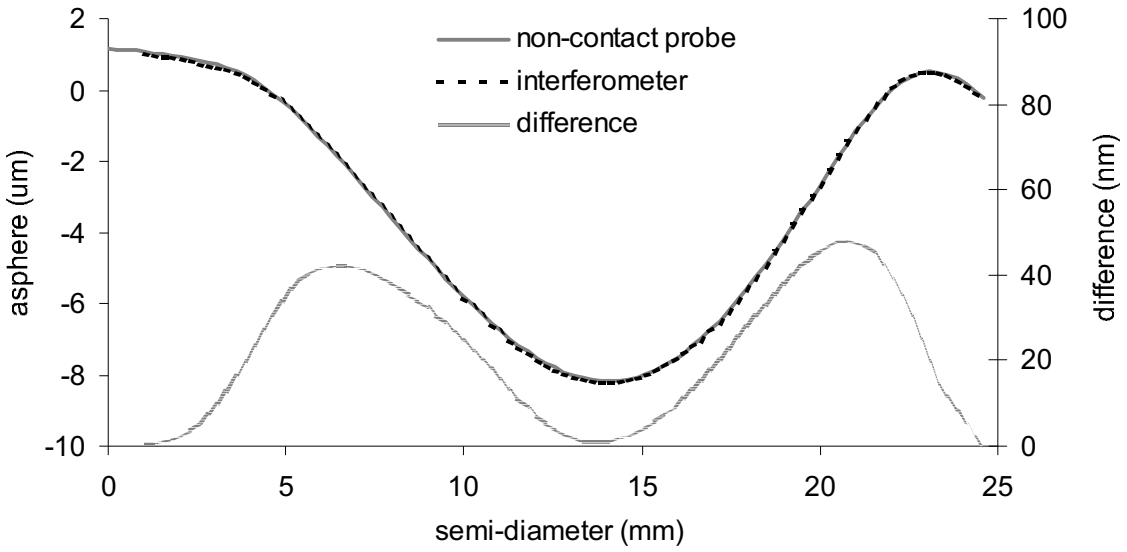

Figure 7: Comparison of non-contact probe and interferometer measurement of asphere on planar surface.

Figure 8 compares the non-contact probe results with an interferometer measurement of a 0.3 μm asphere on a concave spherical surface with a radius of curvature of 88 mm. The measurements agree to within 5 nm of each other. The low frequency sinusoidal difference is an artifact from the air-bearing spindle.

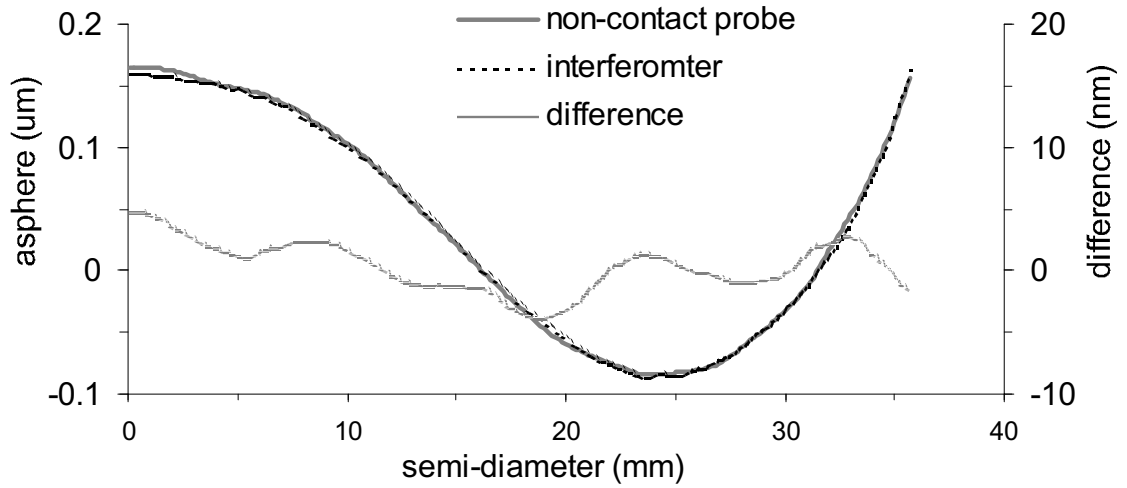

Figure 8: Comparison of non-contact probe and interferometer measurement of asphere on Cc f/1.15 surface.

A 17 μm asphere on a convex surface with a 4300 mm radius was mounted on the linear air bearing and measured with the non-contact probe. It is compared to a 244 nm interferometer measurement using a null lens setup. Figure 9 shows the nominal asphere plotted along with the probe measurement minus nominal and interferometer measurement minus nominal. The measurements agree to within 25 nm of each other. The low order difference is caused by errors in the null lens.

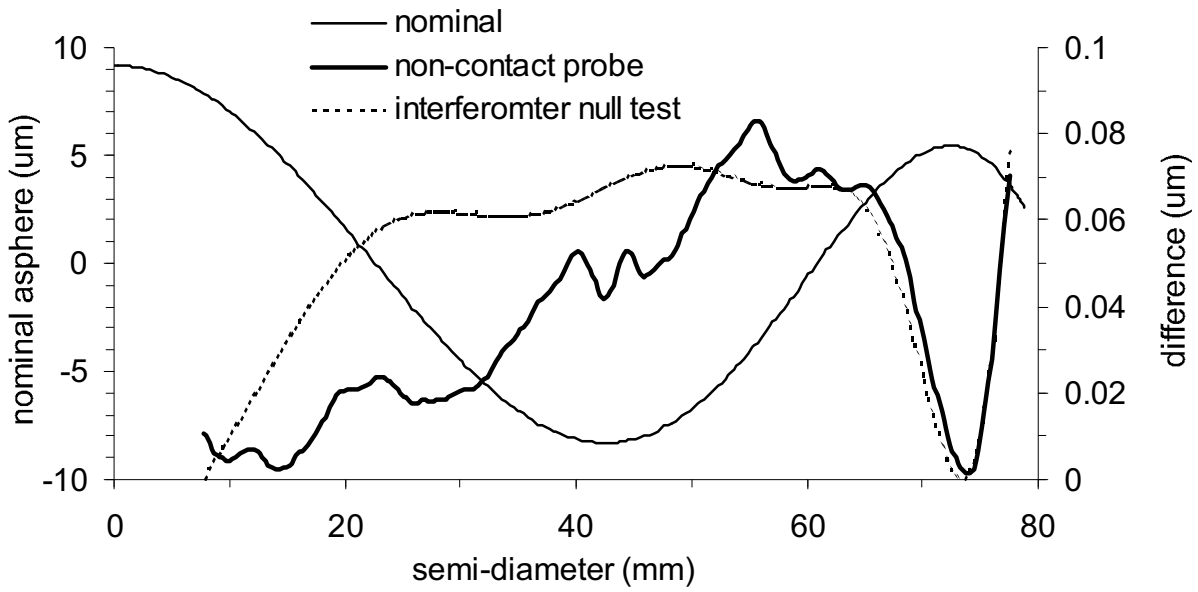

Figure 9: Comparison of non-contact probe and interferometer null test measurement of plano asphere.

6. CONCLUSIONS

Several examples of aspheric surfaces, plano and concave, were measured using the described procedure and compared to interferometer measurements. In one case, the non-contact probe results were compared to null test measurements of a planar aspheric surface. The results proved that it is possible to characterize symmetric aberrations in large departure aspheric surfaces to nearly single digit nanometer precision. Error sources were investigated and demonstrated to be in the single digit nanometer range. Measurement data was low-pass filtered to further reduce noise and vibration thus allowing the non-contact probe to resolve greater than 1 mm spatial features roughly 10-20 nm in height.

REFERENCES

1. P. L. Ruben, "Refractive null correctors for aspheric surfaces," Appl. Opt., **15**, pp. 3080-3083 , 1976.
2. A. Offner and D. Malacara, "Null tests using compensators," in Optical Shop Testing, 2nd ed., D. Malacara, ed. (Wiley, New York, 1992), pp. 427–454.
3. R. Pursel, "Null testing of an f/0.6 concave aspheric surface," Proc. SPIE Vol. 2263, Current Developments in Optical Design and Optical Engineering IV, pp 210-217, 1994.
4. J. G. Dil, P. F. Greve and W. Mesman, "Measurement of steep aspheric surfaces," Appl. Opt., **17**, pp. 553-557, 1978.
5. H. van Brug, M. Melozzi, L. Pezzati, and A. Mazzoni, "Testing aspheric surfaces using multiple annular interferograms," Opt. Eng., **32**, pp. 1073–1079, 1993.
6. B. Dorband and H. J. Tiziani, "Testing aspheric surfaces with computer-generated holograms: analysis of adjustment and shape errors," Appl. Opt., **24**, pp. 2604-2611, 1985.
7. H. Lee and S. Kim, "Precision profile measurement of aspheric surfaces by improved Ronchi test," Opt. Eng., **38**(6), Donald C. O'Shea; Ed., pp. 1041-1047, 1999.
8. A. Handojo and H. J. Frankena, "Testing Aspheric Surfaces: Simple Method with a Circular Stop," Appl. Opt., **37,** pp. 5969-5973, 1998.

9. A. E. Lowman and J. E. Grivenkamp, "Interferometer induced wavefront errors when testing in a non-null configuration," in Interferometry VI: Applications , R. J. Pryptniewicz , G. M. Brown , and W. E. Jeuptner , eds. , Proc. SPIE 2004, pp. 173-181, 1993.
10. C. Huang, "Propagation errors in precision Fizeau Interferometry," Appl. Opt., **32**, pp. 7016-7021, 1993.
11. P. E. Murphy, T. G. Brown and D. T. Moore, "Interference imaging for aspheric surface testing," Appl. Opt., **39**, pp. 2122-2129, 2000.
12. J. D. Lytle and A. L. Palmer, "Aspheric profile gauging using a bootstrap data interpretation technique," Appl. Opt., **18**, pp. 1064 -1070, 1979.
13. K. Yoshizumi, T. Murao, J. Masui, R. Imanaka, and Y. Okino, "Ultrahigh accuracy 3-D profilometer," Appl. Opt., **26**, pp. 1647-1653, 1987.
14. W. Gao and S. Kiyono, "Development of an optical probe for profile measurement of mirror surfaces," Opt. Eng., **36**(12), Brian J. Thompson; Ed., pp. 3360-3366, 1997.
15. Q. Wang, Z. Zhang, X. Zhang, and J. Yu, "Novel profilometer with dual digital length gauge for large aspheric measurements," Proc. SPIE Vol. 4231, Advanced Optical Manufacturing and Testing Technology, pp. 39-46, 2000.
16. A.V. Zvyagin, I.Eix, and D.D. Sampson, "High-speed, high-sensitivity, gated surface profiling with closed-loop optical coherence topography," Appl. Opt., **41**, pp. 2179-2184, 2002.